



Available online at [www.sciencedirect.com](http://www.sciencedirect.com)



Chemical Physics Letters 381 (2003) 53–59

**CHEMICAL  
PHYSICS  
LETTERS**

[www.elsevier.com/locate/cplett](http://www.elsevier.com/locate/cplett)

## Molecular dissociation observed with an atomic wavepacket and parametric four-wave mixing

A.A. Senin <sup>\*</sup>, H.C. Tran <sup>1</sup>, J. Gao, Z.H. Lu, C.J. Zhu, A.L. Oldenburg <sup>2</sup>,  
J.R. Allen, J.G. Eden <sup>\*</sup>

*Laboratory for Optical Physics and Engineering, Department of Electrical and Computer Engineering, University of Illinois,  
1406 W. Green St., Urbana, IL 61801, USA*

Received 31 July 2003; in final form 10 September 2003  
Published online: 14 October 2003

---

### Abstract

We report the observation of the dissociation of an electronically-excited molecule ( $\text{Rb}_2$ ) with an atomic wavepacket and time-delayed parametric four-wave mixing. The dynamics of the molecular dissociation transient are captured by the temporal histories of the relative number densities of the Rb product states, determined by reference to the amplitude and phase of the Fourier (spectral) components of the wavepacket. Clear experimental evidence of the appearance of atomic fragments (7s, 5d, 6p, 4d, and 5p) generated by dissociation is observed in the pressure-dependent temporal behavior of the amplitude of the  $608 \text{ cm}^{-1}$  (7s–5d) wavepacket spectral component.

© 2003 Elsevier B.V. All rights reserved.

---

Dissociation is a fundamental process of molecular dynamics and a detailed understanding of the relevant potential surfaces is crucial to ultimately controlling the products. Toward that end, a major step was taken in the late 1980s when

Zewail and colleagues [1,2] observed the transition state between a bound molecule and specific dissociative exit channels. In femtosecond laser pulse pump–probe experiments, a wavepacket was first produced within an electronic state of the parent molecule and the subsequent appearance of an atomic or molecular fragment was detected by laser-induced fluorescence. However, since fluorescence is an incoherent process, the retrieval of phase information is problematic and obtaining adequate sensitivity poses experimental challenges. Shortly thereafter, Misewich et al. [3,4] at IBM reported monitoring molecular dissociation through photoabsorption by an atomic fragment. Though capable of observing the phase of the

---

<sup>\*</sup> Corresponding authors. Fax: +217-244-5422 (A.A. Senin), +217-244-7097 (J.G. Eden).

E-mail addresses: [asenin@uiuc.edu](mailto:asenin@uiuc.edu) (A.A. Senin), [jgeden@uiuc.edu](mailto:jgeden@uiuc.edu) (J.G. Eden).

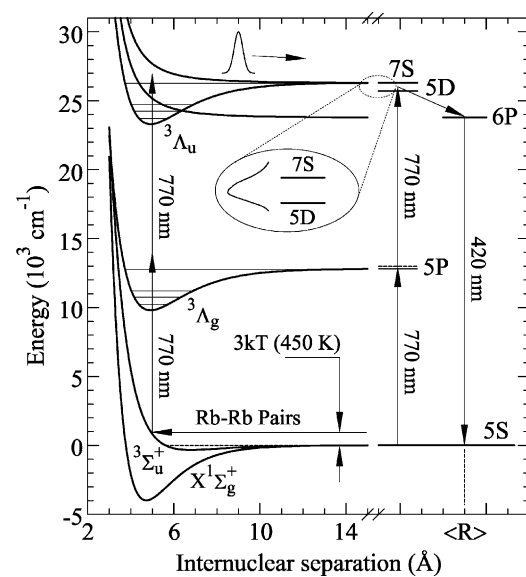
<sup>1</sup> Present address: Northrop-Grumman Corp., 600 Hicks Road, Rolling Meadows, IL 60008.

<sup>2</sup> Present address: Biophotonics Laboratory, Beckman Institute for Science and Technology, University of Illinois, Urbana, IL 61801.

process, absorption measurements record the time-integrated phase and both fluorescence and absorption are limited with respect to selectivity, the ability to simultaneously monitor two or more product states lying close in energy, since either the temporal or spectral resolution of the probe must be compromised.

We report here the detection, with an atomic wavepacket, of the dissociation of an electronically-excited diatomic molecule,  $\text{Rb}_2$  [5,6]. The data presented demonstrate the observation of the molecular dissociation transient and the statistical distribution of product states (spanning more than  $10^4 \text{ cm}^{-1}$ ), unencumbered by collisional or radiative lifetime effects. Specifically, the temporal history of the amplitude and phase of the Fourier (frequency) components comprising the atomic wavepacket provide a stable reference against which the appearance of newly-produced excited atoms can be detected. Rubidium atoms generated by dissociating Rb dimers alter the spatially-averaged, excited state distribution in the medium and, therefore, the third-order nonlinear susceptibility,  $\chi^{(3)}$ . The conversion of this information into the macroscopic domain can be accomplished by parametric four-wave mixing (FWM) in a pump–probe format, which serves to capture the Rb population distribution (among all the states participating in the FWM process) at the moment a probe pulse arrives [7]. Repeated sampling of the medium after the atomic and molecular wavepackets are born and Fourier analysis of the intensity of the coherent signal wave allow one to reconstruct the temporal history and product state distribution of  $\text{Rb}_2$  dissociation. Although molecular and atomic wavepackets have been studied extensively over the past 15 years by a variety of experimental approaches, including photoionization followed by electron or ion detection [8], phase-sensitive techniques [9], and FWM [10,11], they have to date been explored independently. The thrust of this work is to demonstrate the influence of a molecular wavepacket, associated with a dissociating homonuclear molecule, on a coherent nonlinear optical process mediated by an atomic wavepacket.

A potential energy level diagram of the  $\text{Rb}-\text{Rb}_2$  system investigated in these experiments is presented in Fig. 1. Studies of two sets of Rb



pump (and probe), idler and signal, respectively. In 1999, Lvovsky et al. [12] demonstrated that, when excited with 4 ps pulses, the  $5s \rightarrow 5d \rightarrow 6p \rightarrow 5s$  FWM process is time-delayed (idler and signal are generated following the termination of the driving optical field) and the idler is produced by superfluorescence. Nevertheless, the entire process is coherent. In the present experiments, the composition of the wavepacket, reflected by the phase and amplitude of the quantum beating, is embedded in the macroscopic signal wave produced by FWM near the  $6^2P_J \rightarrow 5^2S_{1/2}$  transitions ( $\lambda_s \sim 420$  nm), and is recovered by Fourier analysis of the variation of signal intensity with  $\Delta t$ . The optical pulses for the experiments, having a central wavelength of 770 nm and energies maintained below 1  $\mu$ J, were linearly polarized and generated at a repetition frequency of 1 kHz by a Ti:Al<sub>2</sub>O<sub>3</sub> oscillator–amplifier system. Pairs of pulses separated by a variable time delay ( $\Delta t$ ) were produced with a standard Michelson interferometer and both pulses (spectrally-broadened by self-phase modulation (SPM) in air) were focused into a sapphire cell or heat pipe containing Rb vapor at pressures between  $3.4 \times 10^{-3}$  and 20 Torr (corresponding to number densities, [Rb], of  $\sim 8 \times 10^{13} - 3 \times 10^{17} \text{ cm}^{-3}$ ). The peak optical intensity in the Rb vapor was estimated to be  $\sim 3 \times 10^{10} \text{ W cm}^{-2}$ .

An example of the data obtained by recording the intensity of the coherent emission produced by FWM is shown in Fig. 2 for the  $6p^2P_{3/2} \rightarrow 5^2S_{1/2}$  signal wave ( $\lambda_s \cong 420.19$  nm) in which  $\Delta t$  has been scanned from 0 to 300 ps, and [Rb] is  $\sim 3.7 \times 10^{14} \text{ cm}^{-3}$ . As illustrated by the inset of Fig. 2, the Fourier transform (FFT) of the entire  $\Delta t$ -scan reveals the expected dominant frequency component at  $\sim 608 \text{ cm}^{-1}$ . Because of the length of the scans acquired in these experiments (100–300 ps), identifying unambiguously the fine structure level of  $^2D$  (or  $^2P$ ) states associated with a specific frequency component of a wavepacket is straightforward. In addition to the predominant Fourier component of Fig. 2, nonlinear contributions to the frequency composition of the wavepackets were observed. For interpreting the dynamical data to be presented later, it is important to note here that the measured frequencies of the Fourier components of the wavepacket are within  $\pm 0.08$

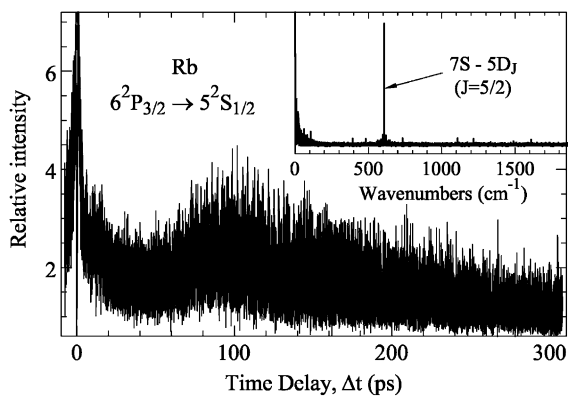


Fig. 2. Representative experimental data illustrating the dependence of the relative intensity of the coherent emission at  $\sim 420.2$  nm ( $6^2P_{3/2} \rightarrow 5^2S_{1/2}$ ) on the pump–probe delay time ( $\Delta t$ ) for  $-10 \lesssim \Delta t \lesssim 300$  ps. The inset shows the FFT of the scan data for which the Rb number density was  $3.7 \times 10^{14} \text{ cm}^{-3}$ .

$\text{cm}^{-1}$  of their accepted values. Therefore, although we have confirmed (with a proportional counter) that photoionization of the atoms by 2+1 resonantly-enhanced multiphoton ionization is saturated at these intensities, the Stark effect has a negligible impact on the temporal history of the wavepacket [13].

As discussed earlier, the interference between the coherent superpositions of the Rb 7s and 5d states produced by the pump and probe pulses serves as the detector of molecular dissociation fragments. A suitable test for this concept requires a process for generating excited molecules in appropriate electronic states (i.e., having dissociative exit channels) and doing so in such a way that the phase with respect to excitation of the atomic wavepacket is well-defined. Both requirements are met by having the pump pulse serve a second function. Returning to Fig. 1, two photon photoassociation [14,15] of thermal pairs of ground state Rb atoms, moving along the  $a^3\Sigma_u^+$  potential [16], excites  $^3\Lambda_u$  ( $\Lambda = \Sigma, \Pi$ , or  $\Delta$ ) states of Rb<sub>2</sub> correlated with  $7^2S$ ,  $5^2D + 5^2S$  in the separated atom limit. Although the Rb<sub>2</sub> electronic states in the two 770 nm-photon region have not been characterized in detail, it is known [17] that several are coupled to the Rb 5p, 4d, ... exit channels by predissociation. Since the same pump pulse photoexcites both atoms and dimers, energetic considerations require

that the molecular wavepacket comprises rovibrational states near the 7s and 5d dissociation limits, and yet also extends into the vibrational continuum. Consequently, the pump pulse establishes, by a two-photon process, a molecular wavepacket on a  $^3\Lambda_u$  potential surface. Dissociation of the dimer results in an excited atomic fragment moving away from its ground state counterpart at a velocity determined by thermal energy and the shape of the interaction potential. In summary, the pump pulse coherently prepares excited molecules which subsequently dissociate, producing atomic fragments entering several exit channels and emerging with specific values of (or, a small spread in) translational energy. It must be emphasized that, *to a first approximation*, excitation of the dimer from the bound ground state ( $X^1\Sigma_g^+$ ) can be neglected in the results described here since: (1) the dimer number density is  $\leq 0.2$ – $1.5\%$  of that for the atom in the Rb vapor pressure range studied ( $3.4 \times 10^{-3}$ – $20$  Torr), and (2) the Rb–Rb photoassociation rate varies as the square of [Rb].

To detect the molecular dissociation transient, the variation of the amplitude and phase of the atomic wavepacket's Fourier components with delay time  $\Delta t$  and [Rb] was determined by analysis of time delay scan data (similar to those of Fig. 2) with the time-dependent Fourier transform. Consider Fig. 3 which compares the temporal histories of the relative amplitude of the  $7\ ^2S_{1/2}$ – $5\ ^2D_{5/2}$  frequency component as the Rb number density is varied by almost four orders of magnitude. Representative data for six values of the vapor pressure are shown and, for clarity, the peak amplitude of the  $608\text{ cm}^{-1}$  Fourier component for each  $\Delta t$ -scan has been normalized to unity. At every pressure studied, a transient increase in the amplitude of the  $608\text{ cm}^{-1}$  signal is observed which is attributed to the interaction of the atomic fragments with the quantum beating process established by the pump in a nearby atom. As the dimers dissociate, the excited fragments acquire a phase shift with respect to the pump pulse that manifests itself as an interference with the 7s–5d oscillator.

As discussed previously, the data of Fig. 3 are not the result of electric field effects resulting from

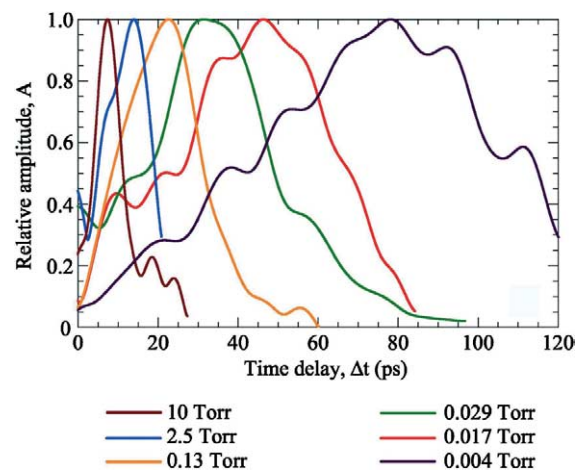


Fig. 3. Dependence of the relative  $7\ ^2S_{1/2}$ – $5\ ^2D_{5/2}$  ( $608\text{ cm}^{-1}$ ) Fourier amplitude on  $\Delta t$  for six values of Rb vapor pressure between  $4 \times 10^{-3}$  and  $10$  Torr ( $9 \times 10^{13} \lesssim [\text{Rb}] \lesssim 1.5 \times 10^{17}\text{ cm}^{-3}$ ). For clarity, the peak amplitude of each of the curves has been normalized to unity. The bandwidth of the integration window in the frequency domain is  $4\text{ cm}^{-1}$ .

electron–ion pairs produced by photoionization. Similarly, over the entire pressure range studied, the transient has terminated long before hard sphere collisions become a factor. Calculations suggest, however, that the falling portion of the transients can be attributed to dephasing of the atomic wavepackets by the dipole–dipole interaction between two excited atoms, one of which is a molecular dissociation fragment. The internuclear separation ( $R$ ) between the two atoms at which the dipole–dipole interaction,  $(\vec{\mu}_1 \cdot \vec{\mu}_2)R^{-3}$ , is  $10$ – $50\%$  of the Rb 7s–5d defect of  $608\text{ cm}^{-1}$  is estimated to be  $120$ – $170\text{ \AA}$ . Assuming that a perturbation of this magnitude is sufficient to destroy the coherence of the wavepacket, this mechanism explains the rate of decay in the amplitude of the transient. We conclude that the influence of dipole–dipole interactions dephases the atomic oscillators (modulating  $\chi^{(3)}$ , the FWM process, and the signal at  $420\text{ nm}$ ) and the  $7\ ^2S$ – $5\ ^2D$  beat frequency amplitude collapses.

More than 100 scans similar to those of Fig. 3, in which the dependence of the  $608\text{ cm}^{-1}$  Fourier component amplitude was recorded for  $0 \leq \Delta t \leq 300\text{ ps}$ , were acquired for several values of [Rb]. The results are presented in Fig. 4a which illus-

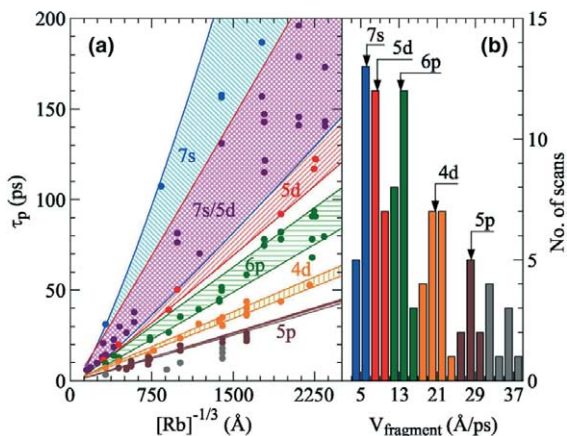


Fig. 4. (a) The variation of  $\tau_p$  with  $[Rb]^{-1/3}$ . The data represent the results of more than 100 scans and the color-coded regions illustrate the predictions of a simple model of the dissociation of electronically-excited dimers in which either a Rb 7s, 5d, 6p, 4d, or 5p fragment is produced. The boundaries of each region, except the low velocity limit for the 7s state, represent Rb–Rb collision (ground state) pairs having energies at the 50% points of a Maxwellian distribution ( $\sim 0.5$  kT and 5.4 kT). The low velocity limit for the 7s state is that for a collision pair energy of 1.2 kT. Considerable overlap exists between the 7s and 5d regions (denoted by the purple cross-hatched pattern) but the 6p, 4d, and 5p regions are distinct. (b) Histogram of the data of (a) but presented here as a function of the velocity of the atomic fragment. The arrows and state labels identify the expected rms velocity (at  $T = 473$  K) for an Rb atom generated in the indicated state.

brates the dependence of  $\tau_p$ , the value of  $\Delta t$  corresponding to the maximum amplitude of a transient, on  $[Rb]^{-1/3}$  which is proportional to the mean separation between Rb atoms for a given number density. These data are in agreement with a simplified picture of the dissociation of electronically-excited  $Rb_2$ . We assume the molecular wavepacket to be produced in a  $^3\Lambda_u$  state (correlated with  $Rb(5^2D \text{ or } 7^2S) + Rb(5^2S_{1/2})$ ) at the value of internuclear separation  $R_0$  for which a colliding pair of Rb ground state atoms, having a center-of-mass kinetic energy  $E_{TH}$ , intercepts the  $^3\Sigma_u^+$  potential. Defining  $\Delta E = E_{TH} + 2\hbar\omega_p - E_{Rb}$  (where  $E_{Rb}$  is the energy of the Rb excited state in question) to be the energy beyond that necessary to access the 7s, 5d, 6p, ... exit channels, accounting for the dipole–dipole interaction noted earlier, and assuming that all of  $\Delta E$  appears as

kinetic energy of the fragments, then the color-coded regions in Fig. 4a show the predicted behavior of the molecular dissociation transients associated with the Rb 7s, 5d, 6p, 4d, and 5p product states. The boundaries of each region (except for the low velocity limit for the 7s fragment – see Fig. 4) correspond to  $E_{TH} \cong 0.5$  kT and 5.4 kT, the 50% points for a Maxwellian distribution. Notice that as thermal energy becomes a smaller fraction of the total excess energy  $\Delta E$  for an atomic fragment, the angular breadth of the region associated with that fragment narrows. Consequently, the 7s and 5d regions of Fig. 4a overlap significantly but those for the 6p, 4d, and 5p fragment states are quite distinct.

A clearer picture of the capability of this experiment to resolve the fragment velocity corresponding to each dissociation channel is provided by the histogram of Fig. 4b. Here, the data of Fig. 4a are categorized with respect to the velocity of the atomic fragment (in  $2 \text{ \AA}/\text{ps}$  increments) and the ordinate gives the number of scans within a particular velocity interval. For convenience, the vertical arrows and state labels identify the calculated rms velocity for the given dissociation exit channel, assuming a  $T = 473$  K Maxwellian velocity distribution for the Rb–Rb collision pairs. The correlation between local maxima in the histogram and the expected velocities for 7s, 5d, 6p, 4d, and even 5p atomic fragments is remarkable and underscores the conclusion that transients associated with the dissociation of  $Rb_2$  and the concomitant generation of atomic fragments have, indeed, been observed. Notice that the observed product states span an energy range of almost  $14000 \text{ cm}^{-1}$ . Also, from a conceptual standpoint, the data of Fig. 4b allow for the branching ratios for the dissociation of electronically-excited  $Rb_2$  into specific states to be estimated. Although these results must be viewed as tentative, the 7s + 5d, 6p, 4d, and 5p yields are determined to be  $(45 \pm 10)\%$ ,  $(27 \pm 10)\%$ ,  $(17 \pm 5)\%$ , and  $(11 \pm 5)\%$ , respectively.

One of the simplifications in the above analysis is that it assumes a single exit channel for each experimental ( $\Delta t$ -scan) run. In reality, one might expect a given dissociation transient to itself be a

sum of transients, each associated with a specific Rb excited state. Indeed, the observed transients do exhibit temporal structure but, for a fixed value of [Rb], variations in the laser pulse chirp and intensity, arising from the SPM process by which we currently generate the necessary bandwidth, influence the dominant exit channel. We have chosen, therefore, to describe each transient by a single maximum at  $\tau_p$  that reflects the *dominant* dissociation pathway.

The ability to detect the dissociation transients of Figs. 3 and 4 by FWM is interpreted in terms of the alteration of the spatially-averaged Rb excited state population by the atomic fragments of Rb<sub>2</sub> dissociation. The initial distribution of population among specific Rb excited states is established by the pump pulse. The subsequent appearance of Rb atoms produced by a second (indirect) source, the dissociation of electronically-excited Rb<sub>2</sub> dimers, modifies that distribution and, hence,  $\chi^{(3)}$  of the medium and the temporal history of the FWM signal radiation. Thus, the *macroscopic* response of the medium will reflect the fact that the distribution of number density among the states associated with the FWM process, integrated over the entire atomic ensemble along the probe pulse path, has been altered in the time interval  $\Delta t$  between the pump and probe pulses. This conclusion is illustrated by considering the expression for the effective wavefunction  $|\Psi\rangle$  of the atomic ensemble:  $|\Psi(t)\rangle = |g\rangle + c_s(t)|s\rangle + c_d(t)|d\rangle + c_p(t)|p\rangle$ , where g represents the ground state of the atom, and s, d, and p denote the primary excited levels participating in the parametric FWM process. Calculating the time-varying coefficients  $c_s$ ,  $c_d$ , and  $c_p$  by first-order perturbation theory and, subsequently, the polarization of the medium ( $\mathbf{P} \propto \langle \Psi(t) | e\mathbf{r} | \Psi(t) \rangle$ ) shows that  $\chi^{(3)}$ , which governs the FWM process when the probe pulse arrives, *incorporates explicitly the relative amplitudes of the s, p, and d states* and includes the quantum beating terms:  $\cos[(\omega_d - \omega_p)\Delta t]$ ,  $\cos[(\omega_s - \omega_p)\Delta t]$ , and  $\cos[(\omega_s - \omega_d)\Delta t]$ . Details of the calculations will be published elsewhere but suffice it to say that the amplitudes of the Fourier components are weighted by the respective populations of the states at any given time delay  $\Delta t$ .

In summary, experiments have been described in which the dissociation of electronically-excited molecules has been observed with an atomic wavepacket and parametric FWM. The data of Figs. 3 and 4, acquired over a range of Rb number density of almost four orders of magnitude, vividly illustrate the detection of a molecular wavepacket associated with dissociating Rb dimers, and the partition of the wavepacket into atomic product states. The fundamental principle underlying the results reported here is that the microscopic production of electronically-excited atoms from molecular dissociation mediates the macroscopic process of generating, via parametric FWM, the coherent signal beam. Since an atomic wavepacket and a coherent optical process (FWM) serve jointly as the detector, the evolving amplitude and phase of the molecular transient can be determined if the pump pulse is well-characterized. It appears that this spectroscopic tool can readily be extended to studying the dissociation of polyatomic molecules in which diatomic (or larger) molecular fragments are produced.

## Acknowledgements

This work was supported by the US Air Force Office of Scientific Research.

## References

- [1] M. Dantus, M.J. Rosker, A.H. Zewail, J. Chem. Phys. 87 (1987) 2395.
- [2] T.S. Rose, M.J. Rosker, A.H. Zewail, J. Chem. Phys. 88 (1988) 6672.
- [3] J.A. Misewich, J.H. Gownia, J.E. Rothenberg, P.P. Sorokin, Chem. Phys. Lett. 150 (1988) 374.
- [4] R.E. Walkup, J.A. Misewich, J.H. Gownia, P.P. Sorokin, Phys. Rev. Lett. 65 (1990) 2366.
- [5] Preliminary results were presented in: P.C. John, H.C. Tran, J.G. Eden, Proc. Annual Mtg. of the IEEE Lasers and Electro-Optics Society, 1996, p. 431.
- [6] A.L. Oldenburg, J.G. Eden, Technical Digest, Conf. on Quantum Electron. and Laser Science (QELS), 1999, p. 176.
- [7] H.C. Tran, P.C. John, J. Gao, J.G. Eden, Opt. Lett. 23 (1998) 70.
- [8] J.A. Yeazell, C.R. Stroud Jr., Phys. Rev. Lett. 60 (1988) 1494.

- [9] N.F. Scherer, R.J. Carlson, A. Matro, M. Du, A.J. Ruggiero, V. Romero-Rochin, J.A. Cina, G.R. Fleming, S.A. Rice, *J. Chem. Phys.* 95 (1991) 1487.
- [10] M. Motzkus, S. Pedersen, A.H. Zewail, *J. Phys. Chem.* 100 (1996) 5620.
- [11] M. Schmitt, G. Knopp, A. Materny, W. Kiefer, *Chem. Phys. Lett.* 270 (1997) 9; *Chem. Phys. Lett.* 280 (1997) 339; *J. Phys. Chem. A* 102 (1998) 4059.
- [12] A.I. Lvovsky, S.R. Hartmann, F. Moshary, *Phys. Rev. Lett.* 82 (1999) 4420.
- [13] M. Strehle, U. Weichmann, G. Gerber, *Phys. Rev. A* 58 (1998) 450.
- [14] See, for example, J.K. Ku, G. Inoue, D.W. Setser, *J. Phys. Chem.* 87 (1983) 2989.
- [15] R.B. Jones, J.H. Schloss, J.G. Eden, *J. Chem. Phys.* 98 (1993) 4317.
- [16] J. Weiner, V.S. Bagnato, S. Zilio, P.S. Julienne, *Rev. Mod. Phys.* 71 (1999) 1.
- [17] F. Spiegelmann, D. Pavolini, J.-P. Daudey, *J. Phys. B* 22 (1989) 2465.